

# Effect of ions on confined near-critical binary aqueous mixtures

Faezeh Pousaneh,<sup>1</sup> Alina Ciach,<sup>1</sup> and Anna Maciołek<sup>2,3,1</sup>

<sup>1</sup>*Institute of Physical Chemistry, Polish Academy of Sciences,*

*Kasprzaka 44/52, PL-01-224 Warsaw, Poland*

<sup>2</sup>*Max-Planck-Institut für Intelligente Systeme,*

*Heisenbergstraße 3, 70569 Stuttgart, Germany*

<sup>3</sup>*Universität Stuttgart, Institut für Theoretische und Angewandte Physik,*

*Pfaffenwaldring 57, 70569 Stuttgart, Germany*

## Abstract

Near-critical binary mixtures containing ions and confined between two charged and selective surfaces are studied within a Landau-Ginzburg theory extended to include electrostatic interactions. Charge density profiles and the effective interactions between the confining surfaces are calculated in the case of chemical preference of ions for one of the solvent components. Close to the consolute point of the binary solvent, the preferential solubility of ions leads to the modification of the charge density profiles in respect to the ones obtained from the Debye-Hückel theory. As a result, the electrostatic contribution to the effective potential between the charged surface can exhibit an attractive well. Our calculations are based on the approximation scheme valid if the bulk correlation length of a solvent is much larger than the Debye screening length; in this critical regime the effect of charge on the concentration profiles of the solvent is subdominant. Such conditions are met in the recent measurements of the effective forces acting between a substrate and a spherical colloidal particle immersed in the near-critical water-lutidine mixture [Nature **451**, 172 (2008)]. Our analytical results are in a quantitative agreement with the experimental ones.

PACS numbers: 05.70.Np, 05.70.Jk, 82.45.Gj

## I. INTRODUCTION

Ions dissolved in a binary liquid mixture often display preferential solubility in the one component of the solvent. Also the interaction between the  $\pm$  ions and the solvent can be different, which is known as an unequal partitioning of ions. In a bulk system, a selective solvation leads to the shift of the critical point of the demixing transition [1–3] and to a number of other effects on the phase separation of a binary solvent [4]. In the presence of external charged surfaces the shift of the bulk critical point of a mixture can be enhanced by a dielectric inhomogeneity arising due to the attraction of high permittivity solvent to the charged surface (dielectrophoretic forces) [5–7]. Moreover, a selective solvation of ions may change the concentration profiles of the binary solvent near the wall and, reversely, adsorption phenomena can significantly influence the distribution of ions near a charged surface. These mutual influences have been recently studied theoretically for the case when the binary solvent is near its consolute point in the semi-infinite geometry [8], and for systems confined between two parallel walls or substrates [9–11]. In the latter case, the consequences of the ions-solvent coupling for the effective forces acting on the confining surfaces were studied.

One of the motivation for such investigations is provided by recent experimental works [12–14], where the effective potential between a charged substrate and a likely charged colloidal particle immersed in a water-lutidine critical mixture ( $T_c \simeq 307.15K$ ) was directly measured. The surfaces of the colloidal particle and of the flat substrate with similar or opposite adsorption preferences were used in order to verify predictions of the theory for the thermodynamic Casimir force. These, so called, critical Casimir forces acting between the colloidal particle and a flat substrate arise as a result of the modifications of the relevant order parameter (OP) and restrictions of its fluctuation spectrum by the confining surfaces. Close to the critical point of the solvent, attraction is predicted for like surfaces, whereas repulsion is predicted if one surface is hydrophilic and the other one is hydrophobic.

The theory of effective interactions between two surfaces confining a near-critical fluid is well developed for uncharged surfaces and for mixtures of neutral components [15–18]. However, in the experiments mentioned above the surfaces were charged, and moreover, a small amount of ions was present in the solution. In Ref. [12, 13] the ions result from dissociation of water, and in Ref. [14] a hydrophilic salt was added. Far from  $T_c$  repulsion

has been present independently of the adsorption preferences of the surfaces, because the electrostatic potential dominates [12–14]. The electrostatic repulsion decays exponentially with the decay rate equal to the Debye screening length  $1/\kappa$ . For  $T \rightarrow T_c$ , in addition to the repulsion for small separations  $L \sim 1/\kappa$ , an attraction (repulsion) has been observed for surfaces with the same (opposite) adsorption preferences for larger separations,  $L \sim \xi$ , where  $\xi$  is the bulk correlation length of the solvent [12, 13]. Such behavior is predicted by the sum of the electrostatic and the critical Casimir potentials for the corresponding boundary conditions. A full quantitative agreement between the experiment and the sum of the electrostatic and the critical Casimir potentials could not be obtained, however [12, 13]. The sum of the electrostatic potential that fitted well the experimental results far from  $T_c$  and of the critical Casimir potential that fitted well the data for separations  $L \gg 1/\kappa$  close to  $T_c$ , for intermediate distances disagreed strongly with the measured potential. The authors concluded that coupling between the critical concentration fluctuations and the distribution of ions may lead to modifications of the potential. For this reason, only distances significantly larger than the screening length were considered close to the critical point to verify the theory of the critical Casimir potential. In the presence of salt a more complex behavior was observed, in particular, an unexpected attraction between hydrophilic and hydrophobic surfaces for intermediate temperatures ( $\xi\kappa < 1$ ) [9–11, 14].

The shape of the effective interaction potentials between charged selective surfaces confining the critical binary solvent with ions resembles strongly the intermolecular interaction potentials, but on a much larger scale. Because of possible applications, the ability to design the interaction potential between, e.g., the two colloidal particles is of interest, therefore the mutual effect of ion distribution and concentration profiles deserves serious attention.

Theoretical studies reported in Refs. [9–11, 19] are all based on the Ginzburg-Landau-like theory but with a different level of complexity as far as the parameter space is concerned. In general, a high-dimensional parameter space is required for a full description of a four-component mixture, with two of the species carrying a charge, in a presence of two charged and selective surfaces. In Refs. [10, 11] the reduced description has been employed in order to investigate the particular mechanisms and the role of the specific interactions. Accordingly, in these studies, e.g., the van der Waals (vdW) type of interactions between ions and between ions and the walls have been neglected altogether. In Ref. [10], a non-trivial interplay between critical and electrostatic phenomena (which goes beyond the simple superposition

of the critical Casimir and the electrostatic potentials) arises as a result of an unequal partitioning of the salt ions in a non-uniform solvent. In Ref. [11], the focus is on the electrostatic effects, therefore also interactions between the components of the solvent and the walls have been neglected. A preference of charged walls for one of the solvent components (with the largest permittivity) has been taken into account via the composition-dependent permittivity. Within this approach, for an equal partitioning of the salt ions in each component of the solvent, an attraction between like-charge surfaces can occur as a result of dielectrophoretic forces and the ion-solvent coupling.

Here we extend the theoretical approach developed in Ref. [8] for a semi-infinite system to the *slit* geometry and determine the influence of critical adsorption on the charge distribution close to the critical point of the solvent, i.e., for  $\kappa\xi > 1$ . Such a ratio of relevant length scales in the system has been realized in the experiments described in Ref. [12, 13]. Next we examine the effect of these modifications of the distribution of ions on the form of the effective potential between confining surfaces which are charged and selective. Within the approximation scheme that we use in our analysis, this effective potential can be written as a sum of three contributions: the critical Casimir potential, the pure electrostatic potential (as given by the linearized Debye-Hückel (DH) theory), and the potential arising from the ion-solvent coupling. We use a Derjaguin approximation [20] in order to compare our theoretical predictions for the effective potential with the experimental data reported in Ref. [12, 13]. Within the Derjaguin approximation the interaction potential between the sphere and the planar wall is expressed in terms of the interaction potential in the slit. For the critical Casimir part of the total effective potential we use the scaling function determined to a great degree of accuracy from the MC simulations in  $d = 3$  [21].

The description of the system used in the present paper is more complete than the ones used in Refs. [10, 11, 19] in the sense that it treats ions as the molecules which interact also non-electrostatically with each other and with the walls. Consequently, we consider a system confined by two charged walls which are selective to *all* components of the mixture. Due to the more complete description, the parameter space of our model is somewhat larger than in the other approaches [10, 11, 19]. In the full version of the model [8], the vdW interactions between all pairs of components of the mixture, and the dependence of the permittivity on the concentration was assumed. The number of parameters can be reduced for particular systems. For example, for hydrophilic ions we are left with 3 parameters

characterizing non-Coulombic interactions [8], while two such parameters are present in Refs. [10, 11]. Rather general description developed from microscopic theory lends itself to still another mechanisms leading to the unintuitive effects in the slit geometry [9]. Moreover, the general framework of our theory is also suitable for antagonistic salt, which leads to interesting phenomena [22]. Finally, because the Ginzburg-Landau-type theory that we employ has been developed from the microscopic lattice gas model of the four-component mixture, in our model the entropy of mixing is better approximated than in Refs. [10, 11], where the entropy of mixing has been taken separately for the binary solvent (without ions) and separately for the ions (as an entropy of an ideal gas). In the present work we assume, as in Ref. [10] a uniform permittivity, because the dielectrophoretic effects can be mimicked by an appropriate contributions to the surface fields. Here we consider the case of the equal partitioning of the ions in the solvent (like in Ref. [11]). What distinguishes our study from the other similar approaches proposed recently, is that our *analytical* results are obtained *beyond* the linear approximation for the EL equations, and a *quantitative*, not only a qualitative agreement with experiments is obtained. As in Ref.[19], interesting effects appear when the nonlinear terms in the EL equations are included.

Our presentation is organized as follows. In Sec. II, we provide the physical background of the phenomena studied in the present work. In Sec. III we describe our model. Approximate, analytical solutions of the Euler-Lagrange equations for the order parameters, valid for  $\kappa\xi > 1$ , are given and discussed in Sec. IV. In Sec. V we obtain results for the effective potential between the confining surfaces. The quantitative comparison with the experimental data are described in Sec. VI. We discuss our results and conclude in Sec. VII.

## II. BACKGROUND

A wall of a container or a surface of a colloidal particle disturb the structure of the fluid in contact with them because of geometrical constraints on the positions of the molecules, and because the molecules interact with the matter of the wall rather than with the fluid molecules that are missing beyond the external surface. Structural changes are present for separations from the surface of the order of the bulk correlation length  $\xi$ . In particular, near a surface preferentially adsorbing one component of the mixture the excess concentration of this component extends to distances  $\sim \xi$ , and for  $T \rightarrow T_c$  (hence  $\xi \rightarrow \infty$ ) this phenomenon

is called critical adsorption [23].

When a second, parallel wall at the separation  $L$  from the first one is present, the excess grand potential of the fluid confined in the slit has the form [24]

$$\Omega_{ex} = \omega_{ex}A = \Omega + pAL = ((\gamma_0 + \gamma_L) + \Psi(L))A \quad (1)$$

where  $A$  is the area of each surface,  $p$  is the bulk pressure and  $\gamma_0$ ,  $\gamma_L$  are the surface tensions at the corresponding walls. The surface tension results from the particle-wall interactions, and from the modification of the structure of the fluid near the single surface in the semiinfinite system. The effective potential  $\Psi(L)$  reflects the mutual effect of both surfaces on the structure of the fluid. The structure of the fluid is influenced simultaneously by both walls if  $L \sim \xi$ , therefore  $\Psi(L)$  vanishes for  $L \gg \xi$ . Since the confined fluid tends to minimize the grand potential,  $\Psi(L)$  and  $-\nabla\Psi(L)$  act as an effective potential and an effective force between the confining surfaces respectively. Close to the critical point associated with either gas-liquid or demixing transition of the confined fluid  $\xi \rightarrow \infty$  and  $\Psi(L)$  acquires a universal contribution which becomes long-ranged at the critical point. This contribution to  $\Psi(L)$  is termed the critical Casimir potential and exhibits scaling described by a universal scaling function which is determined solely by the so-called universality class of the phase transition occurring in the bulk, the geometry, and the surface universality classes of the confining surfaces. The range of  $\Psi(L)$  can be tuned by small temperature changes, because  $\xi = \xi_0\tau^{-\nu}$ , where  $\tau = (T - T_c)/T_c$ ,  $T_c$  is the critical temperature of the solvent, the critical exponent is  $\nu \approx 0.63$  and the system-dependent parameter  $\xi_0$  is of order of a few Angstroms. The theory of the thermodynamic Casimir force [15–18], based on the theory of critical phenomena in confinement [23, 25] is well established. For the Ising universality class in a slit geometry, pertinent to the present study,  $\Psi(L)$  decays exponentially with the decay length equal to the bulk correlation length for distances  $L \gtrsim \xi$ . For the symmetrical (antisymmetrical) surfaces the potential is attractive (repulsive). In the case of a binary mixture, symmetrical (antisymmetrical) surfaces have the same (opposite) adsorption preferences for the components of the binary mixture. Following a convention used commonly in the literature we denote by  $(+, +)$  (and, equivalently,  $(-, -)$ ) the boundary conditions (BC) which reflect the fact that the two surfaces effectively attract the same component of a liquid mixture, whereas  $(+, -)$  BC correspond to the case in which the two surfaces attract different components.

According to the above discussion, one expects the effective critical Casimir interaction

to occur between a colloidal particle and a planar wall or between two colloidal particles immersed in a near-critical binary solvent. Often, in such systems also electrostatic interactions are present, e.g., in colloidal suspensions that are charge-stabilized. The charge at the colloidal particles or at the charged wall is screened by the counterions in the solvent. Accordingly, the electrostatic interactions between two charged colloidal particles or between a colloidal particle and a charged wall become exponential functions of the distance and can compete with the critical Casimir forces. For instance, the effective interaction between charged planar surfaces decays as  $\pm \exp(-\kappa L)$ , where the repulsion (attraction) corresponds to the likely (oppositely) charged surfaces, and the dimensionless inverse Debye screening length is

$$\kappa^* = a\kappa = \sqrt{\frac{4\pi e^2 \rho_c^*}{k_B T \bar{\epsilon}}}. \quad (2)$$

$\rho_c^* = \rho_c a^3$  is the dimensionless number density of ions and  $a$  is the microscopic length unit (we shall choose for  $a$  the size of the solvent molecules). Moreover, this competition can become an interplay. In the present paper we consider charged surfaces immersed in a binary solvent. In such systems, if the solubility of ions in both components of the mixture is the same, then the distribution of charges is independent of the local solvent concentration, and also the concentration of the mixture is not affected by the presence of the ions. As a consequence, the presence of charges at the confining surfaces has no effect on the critical Casimir potential and, vice versa, the critical adsorption has no effect on the electrostatic interactions between the charged surfaces. Therefore  $\Psi(L)$  is just a sum of the critical Casimir and the electrostatic potentials. Usual salts, however, are soluble in water and insoluble in organic liquids. In such a case the critical adsorption of the component preferred by the wall and the distribution of charges may influence each other, and as a result may lead to a different form of  $\Psi(L)$ . The room-temperature critical points are present in mixtures of water and organic liquids, therefore the question how the critical adsorption and the distribution of hydrophilic ions influence each other and modify  $\Psi(L)$  is of practical importance.

### III. GINZBURG-LANDAU THEORY

In this section, following Ref. [8] we briefly summarize the main steps in developing the Ginzburg-Landau theory both from a microscopic lattice gas model and from a continuum one.

#### A. Derivation of the model

In order to obtain the Ginzburg-Landau functional from a continuum microscopic model, one starts from the grand thermodynamic potential of the four-component mixture [24]

$$\Omega = U_{SR} + U_{el} - TS - \int_V d\mathbf{r} \mu_i \rho_i(\mathbf{r}), \quad (3)$$

where  $U_{SR}$  is the energy associated with the short-range (SR) vdW interactions,  $U_{el}$  is the electrostatic energy,  $S$  is the entropy,  $T$  is the temperature and  $\mu_i$  is the chemical potential of the  $i$ -th species. Local dimensionless number densities are denoted by  $\rho_i^*(\mathbf{r}) = \rho_i(\mathbf{r})a^3$ , where  $i = 1, 2, 3, 4$  for water, oil, + and - for ions, respectively. For  $a$  we have chosen the diameter of the organic molecules. In equilibrium,  $\rho_i^*(\mathbf{r})$  correspond to the minimum of  $\Omega$  for given  $T$ ,  $\mu_i$  and the boundary conditions. For ionic species of the same valence,  $\mu_3 = \mu_4 = \mu_c$  because of the charge-neutrality condition. Integration (summation in the lattice version) in Eq. (3) is over the system volume  $V = AL$ , and summation convention for repeated indices is assumed in the whole paper. We assume the usual form of the internal energy  $U_{SR}$ ,

$$U_{SR} = Au_{SR} = \int_V d\mathbf{r} \int_V d\mathbf{r}' \frac{1}{2} \rho_i^*(\mathbf{r}) V_{ij}(\mathbf{r} - \mathbf{r}') g_{ij}(\mathbf{r} - \mathbf{r}') \rho_j^*(\mathbf{r}') \quad (4)$$

$$+ \int_V d\mathbf{r} \rho_i^*(\mathbf{r}) V_i^s(\mathbf{r}),$$

where  $V_{ij}$  and  $g_{ij}$  are the vdW interaction and the pair correlation function between the corresponding components respectively, and  $V_i^s(\mathbf{r})$  is the sum of the direct wall-fluid potentials acting on the component  $i$ . In our model length is in  $a$  units, i.e. we consider dimensionless  $r^* = r/a$  in (4) and in the whole article. However, to simplify the notation we drop the asterisk for  $r$  as well as for the characteristic lengths (like  $\kappa^{-1}$ , see (2)). It should be remembered that length is dimensionless. In the lattice model only nearest-neighbors interact, and the integration in Eq. (4) should be replaced by a summation. In continuum we assume that both the zeroth and the second moments,  $V_0^{(ij)} = \int d\mathbf{r} g_{ij}(r) V_{ij}(r)$  and  $V_2^{(ij)} = \frac{1}{6} \int d\mathbf{r} g_{ij}(r) V_{ij}(r) r^2$ , respectively, are finite.

Compressibility of the liquid can be neglected, so we assume  $\sum_{i=1}^4 \rho_i^* = 1$ . The three independent densities can be chosen as: a concentration of the solvent,

$$s = \rho_1^* - \rho_2^*, \quad (5)$$

a dimensionless density of the solute,

$$\rho_c = \rho_3^* + \rho_4^* \quad (6)$$

(subscript  $c$  from 'charge') and a dimensionless charge density,

$$\phi = \rho_3^* - \rho_4^*. \quad (7)$$

Based on the experimental case where ions in the solution come from dissociation of a water, a similar chemical nature of the anion and the cation is assumed in Ref. [8], and any difference between the interactions of the anion or the cation and any other species is neglected. In the case of salts insoluble in organic liquids the above assumption is not strictly valid, and should be considered as an approximation, whose validity should be verified at the later stage. This assumption distinguishes our analysis from Ref. [10], and has an important consequence for the form of the short-range interaction energy. Namely,  $U_{SR}$  expressed in terms of the new variables depends only on  $s$  and  $\rho_c$ , and is independent of  $\phi$  [8], as can be verified by assuming  $V_{i,3} = V_{i,4}$  in Eq. (4).

The electrostatic energy in a slit with the surface charge  $\sigma(n)$  at the  $n$ -th wall ( $n = 0, L$ ) is

$$\begin{aligned} \frac{U_{el}}{A} = u_{el} = \int_0^L dz \left[ -\frac{\epsilon}{8\pi} (\nabla\psi)^2 + e\phi\psi \right] \\ + e\sigma(0)\psi(0) + e\sigma(L)\psi(L), \end{aligned} \quad (8)$$

where  $e$  is the elementary charge,  $\epsilon$  is the dielectric constant of the solvent and the electrostatic potential  $\psi$  satisfies the Poisson equation,

$$\frac{\epsilon}{4\pi} \frac{d^2\psi(z)}{dz^2} + e\phi(z) = 0. \quad (9)$$

We neglect the dependence of  $\epsilon$  on the solvent concentration for two reasons. Firstly, we take into account that in the critical region the amplitude of the deviations from the average concentration is small and hence such a dependence leads to the higher order corrections to

the order parameter profiles, which we neglect (see Ref. [8] ). Secondly, as already mentioned in the Introduction, the dielectrophoretic effects can be mimicked by an appropriate contributions to the surface fields. Accordingly, while comparing our results with the experimental data we treat the surface fields as the fitting parameters. For an analysis of the dielectrophoretic effects see Refs. [6, 7, 11, 26].

The entropy  $S$  in the lattice model has the form of the ideal mixing entropy. Here we assume the same approximation.

## B. Separation of the charge-dependent and charge-independent parts of the grand potential

The theory of critical phenomena was developed for uncharged systems, therefore we shall separate the part depending on the charge density from the remaining part of the grand potential. For the latter part we shall apply the Ginzburg-Landau description.

In the new variables (Eqs. (6) and (7))  $S$  can be split into two terms,

$$S = -k_B A \sum_{i=1}^4 \int_0^L dz \rho_i^*(z) \ln \rho_i^*(z) = (s_C[s, \rho_c] + s_{el}[\rho_c, \phi])A, \quad (10)$$

with

$$s_C[s, \rho_c] = -k_B \int_0^L dz \left[ \frac{1 - \rho_c(z) + s(z)}{2} \ln \left( \frac{1 - \rho_c(z) + s(z)}{2} \right) + \frac{1 - \rho_c(z) - s(z)}{2} \ln \left( \frac{1 - \rho_c(z) - s(z)}{2} \right) + \rho_c(z) \ln \left( \frac{\rho_c(z)}{2} \right) \right] \quad (11)$$

and

$$s_{el}[\rho_c, \phi] = -k_B \int_0^L dz \left[ \frac{\rho_c(z) + \phi(z)}{2} \ln \left( \frac{\rho_c(z) + \phi(z)}{2} \right) + \frac{\rho_c(z) - \phi(z)}{2} \ln \left( \frac{\rho_c(z) - \phi(z)}{2} \right) - \rho_c(z) \ln \left( \frac{\rho_c(z)}{2} \right) \right]. \quad (12)$$

We use the subscript ' $el$ ' for the quantities that are directly or indirectly associated with electrostatics and vanish for  $\phi = 0$ , and the subscript ' $C$ ' is from "Casimir". From the above properties it follows that the grand potential is a sum of the two terms

$$\Omega = (\omega_C[s, \rho_c] + \omega_{el}[\rho_c, \phi])A \quad (13)$$

where

$$\omega_{el}[\rho_c, \phi] = u_{el}[\phi] - T s_{el}[\rho_c, \phi] \quad (14)$$

and

$$\omega_C[s, \rho_c] = u_{SR}[s, \rho_c] - T s_C[s, \rho_c] - \int_0^L dz \mu_i \rho_i(z) \quad (15)$$

Note that  $s_C[s, \rho_c] + k_B \ln 2 \int_0^L dz \rho_c(z)$  (see Eq. (11)) equals the entropy density of a three-component charge-neutral mixture with the solute density  $\rho_c$  (i.e.,  $\rho_3^* = \rho_4^* = \rho_c/2$ ) and the solvent concentration  $s$  in the case of close packing. Using this observation, one can interpret Eq. (15) as the grand-potential density of such a three-component neutral mixture with  $\mu_c$  replaced by  $\mu_c + k_B T \ln 2$  (recall that  $\mu_c = \mu_3 = \mu_4$ ). Thus, we have separated from the grand potential  $\Omega$  the contribution independent of the charge, which has this advantage that the methods developed for neutral near-critical systems can be directly applied to  $\omega_C[s, \rho_c]$ .

Let us focus on Eq. (14), which can be rewritten as

$$\omega_{el}[\rho_c, \phi] = f_{el}[\rho_c, \phi] - f_{el}[\rho_c, 0] \quad (16)$$

where

$$\begin{aligned} f_{el}[\rho_c, \phi] = & u_{el}[\phi] + k_B T \int_0^L dz \left[ (1 - \rho_c(z)) \ln(1 - \rho_c(z)) \right. \\ & \left. + \frac{\rho_c(z) + \phi(z)}{2} \ln \left( \frac{\rho_c(z) + \phi(z)}{2} \right) + \frac{\rho_c(z) - \phi(z)}{2} \ln \left( \frac{\rho_c(z) - \phi(z)}{2} \right) \right]. \end{aligned} \quad (17)$$

This term alone describes the ions dissolved in a *homogeneous* solvent of the density  $1 - \rho_c$ . However, the two contributions in Eq. (13),  $\omega_C$  and  $\omega_{el}$ , are coupled through  $\rho_c$ . In equilibrium,  $\rho_c(z)$  corresponds to the minimum of  $\Omega$  (Eq. (13)), therefore the critical Casimir and the electrostatic contributions to the effective potential are not independent, even in the case of identical chemical nature of the ions. This implies that the effective potential between the confining walls *must* differ from the sum of the critical Casimir potential and of the electrostatic potential in the case of a homogeneous solvent.

### C. Expansion of the functional

For given  $T$  and  $\mu_i$  the bulk equilibrium densities,  $\bar{s}$ ,  $\bar{\rho}_c$  and  $\bar{\phi} = 0$ , correspond to the minimum of the bulk part of  $\Omega$ ,  $-pAL$ . Deviations of the fields  $s$  and  $\rho_c$  from the bulk

equilibrium values are denoted by

$$\vartheta_1(z) = s(z) - \bar{s} \quad (18)$$

$$\vartheta_2(z) = \rho_c(z) - \bar{\rho}_c \quad (19)$$

where  $z$  is the distance from the left wall. In equilibrium  $\vartheta_1(z)$ ,  $\vartheta_2(z)$  and  $\phi(z)$  correspond to the minimum of  $\omega_{ex}$  (see Eq. (1)). Close to the critical point  $\vartheta_1(z)$ ,  $\vartheta_2(z)$  and  $\phi(z)$  are small for  $z \sim \xi$ , therefore the entropy can be Taylor expanded and the expansion can be truncated. From Eq. (12) we have for fixed  $\bar{\rho}_c$

$$s_{el}[\bar{\rho}_c + \vartheta_2, \phi] = s_{DH}[\phi] + \Delta s[\vartheta_2, \phi] \quad (20)$$

where

$$s_{DH}[\phi] = -k_B \int_0^L dz \left[ \sum_{n \geq 1} a_n \phi^{2n}(z) \right] \quad (21)$$

and

$$\Delta s[\vartheta_2, \phi] = -k_B \int_0^L dz \left[ \sum_{n \geq 1} \sum_{m \geq 1} a_{n,m} \phi^{2n}(z) \vartheta_2^m(z) \right]. \quad (22)$$

The above form follows from the fact that we have chosen to split the total entropy in such a way that  $s_{el}[\rho_c, \phi]$  vanishes for  $\phi = 0$ . The coefficients  $a_n$  and  $a_{n,m}$  resulting from the Taylor expansion of Eq. (12) are functions of  $\bar{\rho}_c$ . The above equations for fixed  $\bar{\rho}_c$  yield

$$\mathcal{L}_{el}[\vartheta_2, \phi] = \omega_{el}[\bar{\rho}_c + \vartheta_2, \phi] = \mathcal{L}_{DH}[\phi] + \Delta \mathcal{L}[\vartheta_2, \phi] \quad (23)$$

where

$$\mathcal{L}_{DH}[\phi] = u_{el}[\phi] + k_B T \int_0^L dz \left[ \frac{\phi^2}{2\bar{\rho}_c} + O(\phi^4) \right] \quad (24)$$

and

$$\Delta \mathcal{L}[\vartheta_2, \phi] = -T \Delta s[\vartheta_2, \phi] = -k_B T \int_0^L dz \left[ \frac{\vartheta_2(z) \phi^2(z)}{2\bar{\rho}_c^2} + O(\vartheta_2^2 \phi^2, \vartheta_2 \phi^4) \right]. \quad (25)$$

As already mentioned, Eqs. (23)-(25) with (8) and (9) describe the ionic system with the charge density  $\phi(z)$  and the total density of ions  $\bar{\rho}_c + \vartheta_2(z)$ , placed between parallel charged walls. When the second term in Eq. (23) is neglected, no excess of the number density of

ions at the surfaces is obtained. It is the term (25) of purely entropic origin that leads to the excess number density of ions near the surfaces [27, 28] when the chemical nature (and hence the interactions with the wall) of the anion and the cation are the same.

From the above considerations it follows that the excess grand potential can be split into three terms,

$$\omega_{ex}[\vartheta_1, \vartheta_2, \phi] \approx \mathcal{L}_C[\vartheta_1, \vartheta_2] + \mathcal{L}_{DH}[\phi] + \Delta\mathcal{L}[\vartheta_2, \phi], \quad (26)$$

where  $\mathcal{L}_C[\vartheta_1, \vartheta_2] = \omega_C[\bar{\rho}_c + \vartheta_2, \bar{s} + \vartheta_1] - \omega_C[\bar{\rho}_c, \bar{s}]$ . Since  $\mathcal{L}_C$  describes the near-critical two-component solvent with addition of one kind of neutral solute, it can be approximated by the Landau-type functional by using standard coarse-graining procedures. Close to the critical temperature  $\vartheta_1(z)$  and  $\vartheta_2(z)$  vary on the length scale large compared to the molecular size, and  $\vartheta_1(z'), \vartheta_2(z')$  can be Taylor expanded about  $z' = z$ . From Eqs. (4) and (11) we thus obtain [8]

$$\mathcal{L}_C = \mathcal{L}_C^0 + k_B T \int_0^L dz \sum_n \sum_m b_{n,m} \vartheta_1^{2n}(z) \vartheta_2^m(z), \quad (27)$$

where in the summation in Eq. (27)  $2n + m \geq 3$ ,  $b_{n,m}$  are functions of  $\bar{\rho}_c$ , and

$$\begin{aligned} \mathcal{L}_C^0[\vartheta_1, \vartheta_2] = & \frac{1}{2} \int_0^L dz \left\{ \vartheta_i(z) C_{ij}^0 \vartheta_j(z) + \nabla \vartheta_i(z) J_{ij} \nabla \vartheta_j(z) \right\} \\ & + \frac{\vartheta_i(0) J_{ij} \vartheta_j(0)}{2} - \bar{h}_i(0) \vartheta_i(0) + \frac{\vartheta_i(L) J_{ij} \vartheta_j(L)}{2} - \bar{h}_i(L) \vartheta_i(L), \end{aligned} \quad (28)$$

where

$$C_{ij}^0 = -J_{ij}^0 - T \frac{\partial^2 s_C}{\partial \vartheta_i \partial \vartheta_j} \Big|_{\vartheta_i=0, \vartheta_j=0}, \quad (29)$$

$J_{ij}^0 = \int d\mathbf{r} J_{ij}(r)$  and  $J_{ij} = \frac{1}{6} \int d\mathbf{r} J_{ij}(r) r^2$ .  $-J_{ij}(r)$  represents the vdW interactions for  $\vartheta_i$  and  $\vartheta_j$ , and can be obtained from the vdW contribution to Eq. (3) with the densities expressed in terms of the new variables (see (5) -(7)). We assume the same interaction ranges for all interacting pairs and postulate  $J_{ij}^0 = 6J_{ij}$  (recall that we consider dimensionless distance). Explicit expressions of  $C_{ij}^0$  are given in Ref. [8] and in Appendix A. Finally,

$$\bar{h}_i(n) = h_i(n) - J_{ij} \vartheta_j(n), \quad (30)$$

where  $h_i(n)$  are the surface fields describing direct interactions with the  $n$ -th wall.  $J_{ij} \vartheta_j(n)$  and the remaining surface terms in Eq. (28) compensate for the interactions with the missing

fluid neighbors due to the presence of the wall; such interactions are present in the bulk term, but should be replaced by the interactions with the molecules of the wall [8].

When the mixture phase separates, both the solvent concentration  $s$  and the density of the solute  $\rho_c$  are different in the coexisting phases, because of a much bigger solubility of the solute in water. Likewise, for  $T$  close to  $T_c$  both  $s$  and  $\rho_c$  exhibit long-range critical fluctuations. Thus, in the Fourier representation the bulk part of  $\mathcal{L}_C^0$  can be written in the form

$$A\mathcal{L}_C^0[\vartheta_1, \vartheta_2] \equiv AL_C^0[\Phi_1, \Phi_2] = \int d\mathbf{k} \frac{1}{2} \left[ \tilde{\Phi}_1(-\mathbf{k}) \tilde{C}_1(k) \tilde{\Phi}_1(\mathbf{k}) + \tilde{\Phi}_2(-\mathbf{k}) \tilde{C}_2(k) \tilde{\Phi}_2(\mathbf{k}) \right] \quad (31)$$

where  $\tilde{C}_i(k)$  and  $\tilde{\Phi}_i(\mathbf{k})$  are the eigenvalue and the eigenvector of  $\tilde{C}_{ij}(k) = C_{ij}^0 + k^2 J_{ij}$ , respectively. The critical order parameter,  $\tilde{\Phi}_1(\mathbf{k})$ , is associated with the eigenvalue  $\tilde{C}_1(k)$  that vanishes at  $T_c$ ;  $\tilde{C}_2(k)$  at  $T_c$  is positive and of the order of unity. The asymptotic decay of correlations in a real space is dominated by  $\tilde{C}_1(0) \propto \xi^{-2}$ . In the critical region, the contribution from the noncritical OP  $\tilde{\Phi}_2(\mathbf{k})$  to the grand potential is much larger than the contribution from the critical OP. Accordingly, the probability of fluctuations associated with  $\Phi_2$  is negligible compared to the probability of the fluctuations corresponding to the critical OP. This allows us to neglect the noncritical fluctuations and  $L_C^0[\Phi_1, 0]$  takes the usual form associated with the critical Casimir potential for the Ising universality class. From the computational point of view, in the present work it is more convenient to consider both fields,  $\vartheta_1$  and  $\vartheta_2$ , instead of their linear combination  $\Phi_1$ .

#### IV. APPROXIMATE SOLUTIONS OF THE EULER-LAGRANGE EQUATIONS

In this section we derive the approximate EL equations for the functional (26) and obtain approximate solutions for the solvent concentration, the solute density and the charge in a slit of width  $L \sim \xi$ . In the one-phase region we neglect the second term in (27), and consider the lowest-order approximation which incorporates the coupling between the critical adsorption and the distribution of charges,

$$\omega_{ex}[\vartheta_1, \vartheta_2, \phi] \approx \mathcal{L}_C^0[\vartheta_1, \vartheta_2] + \mathcal{L}_{DH}[\phi] + \Delta\mathcal{L}[\vartheta_2, \phi]. \quad (32)$$

The first, second and third terms on the RHS of Eq. (32) are given by Eqs. (28), (24) and (25), respectively. We neglect the higher order terms in Eqs. (24) and (25), and in this

approximation the expansion of the functional is truncated at the third order term in the fields  $\vartheta_i$  and  $\phi$ .

The Euler-Lagrange equations, obtained by minimization of the approximate functional (32) with respect to the fields  $\vartheta_i$  and  $\phi$ , together with the Poisson equation (9), take a rather simple form [9],

$$\frac{d^2\vartheta_i(z)}{dz^2} = M_{ij}\vartheta_j(z) + d_i\phi^2(z) \quad (33)$$

$$\frac{d^2\phi(z)}{dz^2} = \kappa^2\phi(z) + \frac{1}{\bar{\rho}_c} \frac{d^2(\phi(z)\vartheta_2(z))}{dz^2}. \quad (34)$$

In the above  $M_{ij} = (J^{-1})_{ik}C_{kj}^0$ , where  $(J^{-1})_{ik}$  is the  $(i, k)$ -th element of the matrix inverse to the matrix  $J_{ij}$  [8], and  $(d_1, d_2) = -\frac{k_B T}{2\bar{\rho}_c^2} \left( (J^{-1})_{12}, (J^{-1})_{22} \right)$ . The solutions must satisfy the charge neutrality condition,

$$\int_0^L dz \phi(z) + \sigma_0 + \sigma_L = 0, \quad (35)$$

and the boundary conditions for  $\vartheta_i$ : [8]

$$\begin{aligned} \frac{d\vartheta_i(z)}{dz} \Big|_{z=0} - \vartheta_i(0) &= H_i(0) \\ -\frac{d\vartheta_i(z)}{dz} \Big|_{z=L} - \vartheta_i(L) &= H_i(L), \end{aligned} \quad (36)$$

where

$$H_i(n) = -(J^{-1})_{ij}\bar{h}_j(n), \quad (37)$$

and  $\bar{h}(n)$  is defined in Eq.(30). For a hydrophilic (hydrophobic) wall  $H_1 < 0$  ( $H_1 > 0$ ). Consistently with the approximate form of the functional (32), the RHS of Eqs. (33) and (34) are truncated at the second order terms.

### A. Solutions of the linearized EL equations

The linearized equations (33) and (34) for  $\vartheta_i$  and  $\phi$  are decoupled. The solutions take the well known forms

$$\phi^{(1)}(z) = -\frac{\kappa\sigma_0}{1 - e^{-\kappa L}} \left( e^{-\kappa z} + R_\sigma e^{-\kappa(L-z)} \right), \quad (38)$$

where we denote the ratio of the surface charges at the two surfaces by

$$R_\sigma = \frac{\sigma_L}{\sigma_0} \quad (39)$$

and use the superscript (1) to distinguish the solutions of the linearized equations. The above charge profile obeys the charge neutrality condition (35). The corresponding approximation for the electrostatic potential is (see linearized Eq. (34), and Eqs. (9), (2))

$$\psi^{(1)}(z) = -\frac{kT}{\bar{\rho}_c} \phi^{(1)}(z). \quad (40)$$

The excess concentration of the solvent and the excess number density of ions (18) in the critical region  $T \rightarrow T_c$  ( $\xi \rightarrow \infty$ ) take the approximate form

$$\begin{aligned} \vartheta_1^{(1)} &= t_0 e^{-z/\xi} + t_L e^{-(L-z)/\xi}, \\ \vartheta_2^{(1)} &= n_0 e^{-z/\xi} + n_L e^{-(L-z)/\xi}. \end{aligned} \quad (41)$$

Because in the critical region the decay length  $\lambda^{-1}$  associated with the larger eigenvalue  $\tilde{C}_2(0) \propto \lambda^2$  is negligible compared to  $\xi$ , the terms  $\propto e^{-\lambda z}$  are subdominant and can be omitted for slits with  $L \gg a$ . From the boundary conditions we obtain the approximate expressions

$$\begin{aligned} n_0 &\simeq n_{01} \frac{1 - CR_n e^{-L/\xi}}{1 - C^2 e^{-2L/\xi}} \\ n_L &\simeq n_{01} \frac{R_n - C e^{-L/\xi}}{1 - C^2 e^{-2L/\xi}} \\ t_0 &\simeq t_{01} \frac{1 - CR_t e^{-L/\xi}}{1 - C^2 e^{-2L/\xi}} \\ t_L &\simeq t_{01} \frac{R_t - C e^{-L/\xi}}{1 - C^2 e^{-2L/\xi}} \end{aligned} \quad (42)$$

where

$$C = \frac{(\xi - 1)}{(\xi + 1)} \quad (43)$$

and

$$\begin{aligned} n_{01} &= \frac{-H_2(0)\xi}{(\xi + 1)} \simeq_{\xi \rightarrow \infty} -H_2(0), & t_{01} &\simeq_{\xi \rightarrow \infty} -H_1(0), \\ R_n &= \frac{H_2(L)}{H_2(0)}, & R_t &= \frac{H_1(L)}{H_1(0)}. \end{aligned} \quad (44)$$

We note that the decoupling of the fields  $\vartheta_2$  and  $\phi$  that occurs after linearization of EL equations is rather unphysical. Nonlinear terms are necessary in order to regain the right physics.

## B. Leading-order corrections in the critical region

In this section we determine the leading-order corrections to the solutions of the linearized EL equations (38) and (41). In Ref. [8] it was assumed that except from distances  $\sim a$  from each wall the dimensionless fields  $f = \vartheta_i, \phi$  are all of the same order of magnitude,  $f = O(\nu)$ , where  $\nu$  is a small parameter.  $\vartheta_i$  and  $\phi$  are proportional to  $H_i$  and  $\sigma$  respectively, thus the analysis in Ref. [8] is restricted to the surfaces with  $H_i, \sigma = O(\nu)$ . Under the above assumption analytical solution of the EL equations can be obtained by systematic approximations within a perturbation method. Since the RHS of Eqs. (33) and (34) are truncated according to the truncation of the functional  $\omega_{ex}$  (see (32)), in a consistent approximation the solutions should have the form  $\vartheta_i = \vartheta_i^{(1)} + \vartheta_i^{(2)}$  and  $\phi_i = \phi_i^{(1)} + \phi_i^{(2)}$ . The superscript (2) refers to the leading order correction terms (of order  $O(\nu^2)$ ), which satisfy the linear inhomogeneous equations

$$\frac{d^2 \vartheta_i^{(2)}(z)}{dz^2} = M_{ij} \vartheta_j^{(2)}(z) + d_i (\phi^{(1)}(z))^2 \quad (45)$$

$$\frac{d^2 \phi^{(2)}(z)}{dz^2} = \kappa^2 \phi^{(2)}(z) + \frac{1}{\bar{\rho}_c} \frac{d^2 (\phi^{(1)}(z) \vartheta_2^{(1)}(z))}{dz^2}. \quad (46)$$

In the above  $\phi^{(1)}$  and  $\vartheta_i^{(1)}$  are given by Eqs. (38) and (41) respectively. The boundary conditions are  $d\vartheta_i^{(2)}(z)/dz|_{z=0} = \vartheta_i^{(2)}(0)$ ,  $d\vartheta_i^{(2)}(z)/dz|_{z=L} = -\vartheta_i^{(2)}(L)$  and  $\int_0^L dz \phi^{(2)}(z) = 0$ , because  $\vartheta_i^{(1)}$  obey Eqs. (36), and  $\phi^{(1)}$  obeys the charge neutrality condition (35). Note that because the Poisson equation (9) is linear, from the above and (2) we obtain the leading-order correction to the electrostatic potential

$$\psi^{(2)} = \frac{k_B T}{e \bar{\rho}_c} \left[ \frac{\vartheta_2^{(1)} \phi^{(1)}}{\bar{\rho}_c} - \phi^{(2)} \right]. \quad (47)$$

Note that in a semiinfinite system the second term on the RHS in Eq. (45) decays as  $\sim \exp(-2\kappa z)$ , and the second term on the RHS in Eq. (46) decays as  $\sim \exp(-\kappa z) \exp(-z/\xi)$ . Further approximations are possible when one of the two length scales, either the correlation  $\xi$  or the screening length  $1/\kappa$ , is much larger than the other length. Following Refs. [8, 9] we introduce the ratio between the correlation and the screening lengths,

$$y = \kappa \xi, \quad (48)$$

and focus on the two limiting cases: (i)  $y \ll 1$ , i.e., the Debye length is much larger than the correlation length, and (ii)  $y \gg 1$ , i.e., the Debye length is much smaller than the correlation length. The analysis of the limiting cases can be done with a reasonable effort. We should note that the experiments showing unusual attractive effective potential between the charged colloidal particle and the charged wall having the opposite adsorption preferences, were performed for  $y < 1$  [14], whereas the experiments reported in Ref. [12, 13] concern the case  $y > 1$ .

Let us first focus on the case (i), which was studied in Ref. [9]. For  $y \ll 1$ , from Eq. (41) we have  $\vartheta_i(1/\kappa) \sim \exp(-1/y) \ll 1$ , and the second term on the RHS of Eq. (34) can be neglected. As a result we obtain that  $\phi \approx \phi^{(1)}$ , and  $\vartheta_i$  satisfy Eqs. (33) and (36). The solution of Eq. (33) with  $\phi \approx \phi^{(1)}$  yields a qualitative agreement with the experimental results for the effective potential obtained for a system with the Debye length larger than the correlation length [14].

The case (ii) was studied in Ref. [8] for a semiinfinite system. For  $y \gg 1$  in the semiinfinite system we have (see Eq. (38))  $(\phi^{(1)}(\xi))^2 \sim \exp(-2y) \ll 1$ . Thus for  $z \sim \xi$  the second term on the RHS of Eqs. (33) and (45) is subdominant with respect to the second term on the RHS of Eq. (46) decaying as  $\sim \exp(-\kappa z) \exp(-z/\xi) \sim_{|z \sim \xi} \exp(-y - 1)$ . Therefore, in the asymptotic region of  $y \gg 1$  we neglect the former but keep the latter. This means that we can approximate the concentration and the number density of ions by the solutions of the linearized EL equations  $\vartheta_i \approx \vartheta_i^{(1)}$ , but we cannot do it for the charge density  $\phi$ . In physical terms the effect of the charge profile on the critical adsorption is negligible for  $y \gg 1$ , because the neutralizing charge in the fluid is present at the distances from the surface  $z \sim \kappa^{-1} \ll \xi$ ; the charge distribution can be neglected on the same footing as the distribution of molecules at the distance  $\lambda^{-1}$  from the wall.

In this work we focus on the case of  $y > 1$ , and adopt the approximation valid in the asymptotic region  $y \gg 1$ . We neglect the effect of the charge distribution on  $\vartheta_1$  and  $\vartheta_2$ , and obtain the leading-order correction to the charge profile from the approximate equation (46). The solution of Eq. (46) can be written in the form

$$\begin{aligned} \phi^{(2)}(z) = \frac{\kappa\sigma_0}{\bar{\rho}_c(1 - e^{-\kappa L})} & \left[ \mathcal{A}_0 e^{-\kappa z} + \mathcal{A}_L e^{-\kappa(L-z)} + \mathcal{A}_{00} e^{-\kappa z} (1 - e^{-z/\xi}) + \mathcal{A}_{0L} e^{-\kappa z} (1 - e^{-(L-z)/\xi}) \right. \\ & \left. + \mathcal{A}_{LL} e^{-\kappa(L-z)} (1 - e^{-(L-z)/\xi}) + \mathcal{A}_{L0} e^{-\kappa(L-z)} (1 - e^{-z/\xi}) \right]. \end{aligned} \quad (49)$$

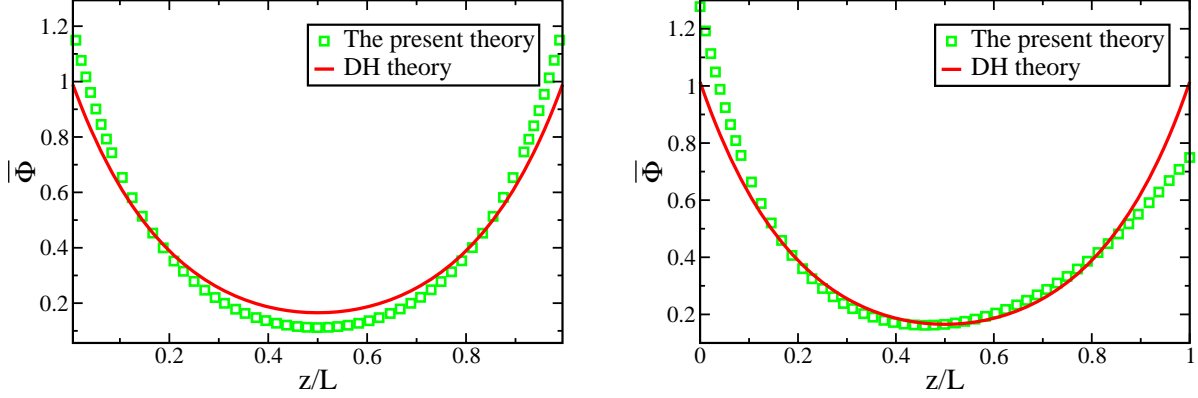


FIG. 1: Charge density profile as a function of the scaled distance  $z/L$ . The solid line represents  $\phi^{(1)}(z)$  (Eq. (38), linearized DH theory result) and the dotted line is the approximate charge density, Eq. (50), with the effect of the critical adsorption included.  $\kappa\xi = 5$ ,  $\kappa L = 5$ ,  $R_\sigma = |R_n| = 1$  (the same charge densities and the same or opposite adsorption preferences at both surfaces), and the excess number density of ions at the surface is  $n_{01} = 0.5$ . Charge density is in  $(-\kappa\sigma_0)$  units. Panels (a) and (b) correspond to the boundary conditions  $(-, -)$  and  $(-, +)$  respectively.

The coefficients are functions of  $y$ ,  $n_0$ ,  $n_L$  and  $R_\sigma$ , and their explicit forms are given in Appendix B. The obtained approximation for the charge density

$$\phi(z) \approx \phi^{(1)}(z) + \phi^{(2)}(z) \quad (50)$$

is shown in Figs. 1(a) and (b) for  $(-, -)$  and  $(-, +)$  boundary conditions, respectively; results correspond to  $y = \kappa L = 5$ .

## V. THE EFFECTIVE POTENTIAL

The main goal of this work is a determination of the effective potential  $\Psi(L)$  between the surfaces that are both selective and charged. From Eq. (32) it immediately follows that the effective potential can be approximated by the sum of the Casimir and the electrostatic potentials only when the last term in (32) is neglected. When the chemical nature of the anion and the cation is the same, this term is of a purely entropic origin.

When  $\Delta\mathcal{L}[\vartheta_2, \phi]$  in Eq. (32) is neglected, then the Casimir and the electrostatic terms are decoupled, and the concentration of the solvent and the solute density are obtained by the minimization of  $\mathcal{L}_C[\vartheta_1, \vartheta_2]$ , whereas the charge profile is obtained by the minimization of  $\mathcal{L}_{DH}[\phi]$  (with a simultaneous solution of the Poisson equation (9)).

When the last term in Eq. (32) is taken into account, it directly yields an extra contribution to the effective potential. What is important, this term depends on both,  $\kappa$  and  $\xi$ , as well as on the surface charges and the surface fields. In addition, when  $\Delta\mathcal{L}[\vartheta_2, \phi]$  is included, then the electrostatic contribution is  $\mathcal{L}_{DH}[\phi^{(1)} + \phi^{(2)}]$  rather than  $\mathcal{L}_{DH}[\phi^{(1)}]$  obtained in the absence of the critical adsorption. This term also depends on  $\xi$  and the surface fields through  $\phi^{(2)}$  (see (49)). We stress again that for a homogeneous solvent  $\Delta\mathcal{L}[\vartheta_2, \phi]$  leads to the excess number density of ions in the layer of thickness  $1/(2\kappa)$  [27, 28]. Neglecting this term leads to an oversimplified theory already for a homogeneous solvent.

In this section we determine the form of the potential  $\Psi(L) = \omega_{ex} - \gamma_0 - \gamma_L$  by substituting to Eq. (32) the approximate forms of the fields  $\vartheta_i \approx \vartheta_i^{(1)}$  (Eq. (41)) and  $\phi \approx \phi^{(1)} + \phi^{(2)}$  (see Eqs. (38) and (49)). The expression for  $\omega_{ex}[\vartheta_1, \vartheta_2, \phi]$  simplifies greatly when the fields  $\vartheta_1, \vartheta_2, \phi$  satisfy the EL equations. For the Casimir part we obtain in our MF approximation

$$\Psi_C = \mathcal{L}_C^0 - \gamma_C(0) - \gamma_C(L) \approx A_C \xi^{-1} e^{-L/\xi}, \quad (51)$$

where  $A_C = -4H_i(0)J_{ij}H_j(L)$  (see Eq.(37)). The remaining contribution to  $\omega_{ex}$  in the approximation consistent with Eq. (32) can be written in the form (see (23))

$$\mathcal{L}_{el} = \Psi_{el}(L) + \gamma_{el}(0) + \gamma_{el}(L) \approx \mathcal{L}_{el}^{(1)} + \mathcal{L}_{el}^{(2)}. \quad (52)$$

The leading order term ( $O(\nu^2)$ ) is given by Eq. (24) with  $\phi$  and  $\psi$  approximated by the solutions  $\phi^{(1)}$  and  $\psi^{(1)}$  of the linearized equations,

$$\begin{aligned} \mathcal{L}_{el}^{(1)} = \int_0^L dz \left[ \frac{k_B T}{2\bar{\rho}_c} \phi^{(1)2} - \frac{\bar{\epsilon}}{8\pi} \left( \nabla \psi^{(1)} \right)^2 + e\phi^{(1)}\psi^{(1)} \right] \\ + e\sigma_0 [\psi^{(1)}(0) + R_\sigma \psi^{(1)}(L)]. \end{aligned} \quad (53)$$

The well-known solutions are

$$\beta\gamma_{el}^{(1)}(n) = \frac{\kappa\sigma_n^2}{2\bar{\rho}_c} \quad (54)$$

and

$$\beta\Psi_{el}^{(1)} = \beta\Psi_{DH} = \frac{\kappa\sigma_0\sigma_L}{\bar{\rho}_c} \left[ \coth\left(\frac{\kappa L}{2}\right) - 1 \right]. \quad (55)$$

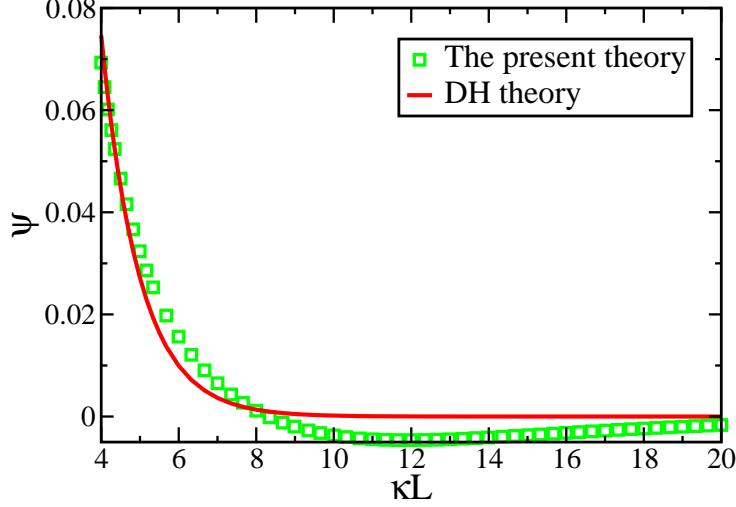


FIG. 2: The contribution to the effective potential per unit area associated with the presence of charges,  $\Psi = \Psi_{el}^{(1)} + \Psi_{el}^{(2)}$  (Eqs. (55) and (58)) for  $(-, -)$  BC as a function of the scaled distance  $\kappa L$  (dotted line). Solid line is the potential  $\Psi_{el}^{(1)}$  resulting from the linearized DH theory. The potential is in units of  $\left[\frac{\kappa\sigma_0^2 k_B T}{2\bar{\rho}_c}\right]$ .  $\kappa\xi = 5$ ,  $R_\sigma = R_n = 1$  and  $n_{01} = 0.5$  (see Eqs.(39) and (44)).

The leading-order correction term is of the order  $O(\nu^3)$ , and has the explicit form

$$\begin{aligned} \mathcal{L}_{el}^{(2)} = & \int_0^L dz \left[ -\frac{k_B T}{2\bar{\rho}_c^2} \phi^{(1)2} \vartheta_2^{(1)} + \frac{k_B T}{\bar{\rho}_c} \phi^{(1)} \phi^{(2)} - \frac{\bar{\epsilon}}{4\pi} \nabla \psi^{(1)} \nabla \psi^{(2)} + e(\phi^{(1)} \psi^{(2)} + \phi^{(2)} \psi^{(1)}) \right] \\ & + e\sigma_0 [\psi^{(2)}(0) + R_\sigma \psi^{(2)}(L)] \end{aligned} \quad (56)$$

By using Eqs. (40) and (47), integrating by parts and after some algebra we obtain

$$\begin{aligned} \mathcal{L}_{el}^{(2)} = & -\frac{k_B T}{2\bar{\rho}_c^2} \int_0^L dz \phi^{(1)2} \vartheta_2^{(1)} \\ & + e\psi^{(2)}(L) \left( R_\sigma \sigma_0 + \frac{\nabla \phi^{(1)}(L)}{\kappa^2} \right) + e\psi^{(2)}(0) \left( \sigma_0 - \frac{\nabla \phi^{(1)}(0)}{\kappa^2} \right), \end{aligned} \quad (57)$$

where the first term equals  $\Delta \mathcal{L}[\vartheta_2^{(1)} \phi^{(1)}]$ . The remaining terms come from  $\mathcal{L}_{DH}[\vartheta_2^{(1)}, \phi^{(1)} + \phi^{(2)}]$ . (The full expression for  $\mathcal{L}_{el}^{(2)}$  is given in Appendix C.)

We neglect terms  $O(\exp(-2L/\xi), \exp(-2\kappa L))$ , and after subtracting the surface-tension contributions, we obtain the approximation

$$\beta \Psi_{el}^{(2)} \approx -\frac{\kappa \sigma_0 \sigma_L n_{01}}{2\bar{\rho}_c^2} \left\{ A_1(y) e^{-L/\xi} + A_2(y) e^{-\kappa L} + A_3(y) e^{-L/\xi} e^{-\kappa L} \right\} \quad (58)$$

where the coefficients are (see Eqs. (39), (44) and (48))

$$A_1(y) = \frac{R_\sigma^2 + R_n}{R_\sigma} \left( \frac{y}{2y - 1} \right) \quad (59)$$

$$A_2(y) = (1 + R_n) \left( \frac{4y^2 + 4y}{2y + 1} \right) \quad (60)$$

$$A_3(y) = -4(1 + R_n) \left( \frac{4y^3 - 2y}{4y^2 - 1} \right). \quad (61)$$

The above approximation is valid for finite  $y$ ; for  $y \rightarrow \infty$  it is not justified to neglect terms  $O(\exp(-2L/\xi))$ , and the approximation (32) is oversimplified. The case relevant for the experiments in Ref. [12, 13], however, corresponds to  $1 < y \lesssim 10$ . The effective potential  $\Psi_{el}^{(1)} + \Psi_{el}^{(2)}$  (Eqs.(55) and (58)) is shown in Fig. 2 for  $(-, -)$  BC. A similar electrostatic attraction between likely charged surfaces was found in Ref.[11] in a nonlinear theory for large  $\kappa\xi$ .

The final approximate expression for the potential per unit surface area of the slit, in the region accessible in these experiments takes the form

$$\beta\Psi(L) \approx \mathcal{D}_1(y)e^{-L/\xi} + \mathcal{D}_2(y)e^{-\kappa L} + \mathcal{D}_3(y)e^{-\kappa L}e^{-L/\xi} \quad (62)$$

where (see Eq.(44))

$$\mathcal{D}_1(y) = A_C \xi^{-1} - \frac{\kappa\sigma_0\sigma_L n_{01}}{2\bar{\rho}_c^2} A_1(y) \quad (63)$$

$$\mathcal{D}_2(y) = \frac{2\kappa\sigma_0\sigma_L}{\bar{\rho}_c} \left[ 1 - \frac{n_{01}}{4\bar{\rho}_c} A_2(y) \right] \quad (64)$$

$$\mathcal{D}_3(y) = -\frac{\kappa\sigma_0\sigma_L n_{01}}{2\bar{\rho}_c^2} A_3(y). \quad (65)$$

In Eqs.(63)-(65) the excess number density of ions at one surface,  $n_{01} = -H_2(0)$ , and the number density of ions in the bulk,  $\bar{\rho}_c$ , have the dimension of  $1/volume$ , surface number densities of elementary charges,  $\sigma_0, \sigma_L$  have the dimension of  $1/area$  (see Eq.(8)), and the inverse Debye and correlation lengths,  $\kappa$  and  $1/\xi$  respectively, as well as the amplitude  $A_C$ , have the dimension of  $1/length$ .

The above MF result can be corrected, because as noted in Sec. III B the Casimir contribution to the potential can be considered separately, and the critical fluctuations can be incorporated in this part. The universal scaling function of the critical Casimir force has been obtained in Monte Carlo simulations [21]. The amplitude  $A_C$  characterizing the long-distance decay of the potential has been extracted from the asymptotic behavior of this function for  $L/\xi \gg 1$  in Ref.[13]. In the case of the symmetrical BC ((+,+) or (-,-))  $A_C = A_+/\xi = -1.51(2)/\xi$ , and in the case of the antisymmetrical BC ((+,-) or (-,+))  $A_C = A_-/\xi = 1.82(2)/\xi$  [13].

Important consequence of the coupling between the critical adsorption and charge distribution is the dependence of the prefactors in Eq.(62) on the ratio between the correlation and the screening lengths,  $y$ .

## VI. COMPARISON WITH THE EXPERIMENT

### A. Derjaguin approximation

The theory developed in the previous sections concerns confining surfaces that are planar and parallel to each other, whereas the measurements in Refs. [12, 13] with which we would like to compare our findings were performed for a planar substrate and a spherical colloidal particle. When the colloidal particle radius is much larger than the separation of its surface from the substrate, then the Derjaguin approximation can be applied, as in Refs.[12, 13]. The curved surface is approximated by a set of concentric circular rings of the infinitesimal area  $dS(\theta)$ . The rings are parallel to the substrate and are at the normal distance  $L(\theta) = z + R(1 - \cos \theta)$  (Fig. 3). For each ring the excess grand potential per unit area is given in Eq. (62), except that the surface charge  $\sigma_R$  of the ring differs from  $\sigma_P$  of the colloidal particle, and the relation between them is

$$\sigma_R = \sigma_P / \cos \theta. \quad (66)$$

Consequently, the ratio between the surface charge at the substrate and at the ring is related to the corresponding ratio between the surface charge at the substrate and the particle by

$$R_{\sigma[w/R]} = R_{\sigma[w/P]} \cdot \cos \theta, \quad (67)$$

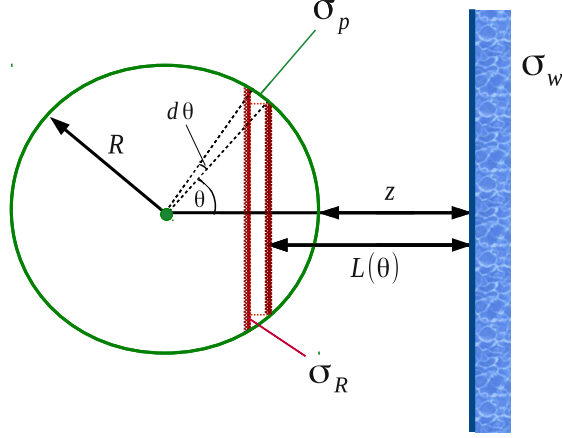


FIG. 3: Illustration of the Derjaguin approximation for the plate-sphere geometry.  $\sigma_P$ ,  $\sigma_R$ ,  $\sigma_w$  are the charge density of the spherical particle, of the ring, and of the wall respectively.  $z$  is the minimal separation between the surface of the colloid and the planar wall.  $L(\theta)$  is the normal distance between the ring and the wall.

where the symbols  $w, P, R$  denote the wall, the colloidal particle and the ring, respectively. The contribution of the ring to the potential between the substrate and the particle has the form

$$d\hat{\Psi}(z) = dS(\theta)\Psi(L(\theta)) \quad (68)$$

where  $dS(\theta)$  is the area of the infinitesimal ring. Finally, the total potential  $\hat{\Psi}(z)$  is obtained by summing all the contributions  $d\hat{\Psi}(z)$  of the circular rings up to the maximal angle  $\theta_M = \pi/2$ ,

$$\hat{\Psi}(z) = \int_0^{\theta_M} dS(\theta)\Psi(L(\theta)) \quad (69)$$

or

$$\hat{\Psi}(z) = \int_0^{\pi/2} 2\pi R^2 \sin \theta \cos \theta \Psi(z + R(1 - \cos \theta)) d\theta \quad (70)$$

## B. Fitting

In this section we shall compare the predictions of our theory with the experiments reported in Ref. [12, 13]. In the experiment one surface was a charged surface of a particle, and the second surface was a flat, likely charged substrate chemically treated to achieve a desired adsorption preference.

Although the theory developed here is of the mean-field type, the Renormalization Group (RG) results can be applied to the Casimir part according to the discussion in Sec. III B. We shall assume that the general form of the potential, Eq. (62), is a fair approximation, except that the correlation length should have the correct temperature dependence,  $\xi = \xi_0 \tau^{-\nu}$ , i.e., with  $\nu$  taking the three-dimensional value 0.63 of the Ising universality class. Moreover, we shall assume that the Casimir amplitude  $A_C$  is given by the proper universal form associated with the Ising universality class.

We shall compare our predictions with the experiment for all four pairs of the boundary conditions:  $(+, +)$ ,  $(-, -)$ ,  $(+, -)$  and  $(-, +)$ , where  $(+)$  denotes a hydrophobic and  $(-)$  denotes a hydrophilic surface; the left and the right symbol in the pair refer to the particle and the substrate respectively. Unfortunately, neither the charge density  $\sigma_w \equiv \sigma_L$  nor the surface fields  $H_i(L)$ ,  $i = 1, 2$  could be measured experimentally. Two kinds of colloidal particles were used: a hydrophilic with the unknown charge density and the radius  $R = 1200(nm)$ , and a hydrophobic with the radius  $R = 1850(nm)$ . The surface fields  $H_i(0)$ ,  $i = 1, 2$  characterizing the colloidal particles are also unknown. According to the experimental conditions we assume that the surface charge  $\sigma_P \equiv \sigma_0$  and the surface fields for the colloidal particles of the same type are fixed. We thus impose strict constraints on  $H_2(0)$  and  $\sigma_0$  to take on the same values for  $(+, +)$  and  $(+, -)$  BC, and the same values (but of course different than in the previous case) for  $(-, -)$  and  $(-, +)$  BC. The same constraints are imposed for the parameters that describe the flat surfaces, i.e., we require that  $\sigma_L = \sigma_0 R_\sigma$  and  $H_2(L) = H_2(0) R_n$  are the same for  $(-, -)$  and  $(+, -)$  BC, and likewise the same for  $(+, +)$  and  $(-, +)$  BC.

In experiments of Refs. [12, 13], ions in the solution were present due to water dissociation in a salt free water-lutidine mixture. For this mixture, according to Ref. [29] the density of (monovalent) ions is about  $\bar{\rho}_c \simeq 1.08 \cdot 10^{-3} mol/l$ . We use this value, although it appears to be a rather rough estimate, and consider  $\kappa$  as a fitting parameter.

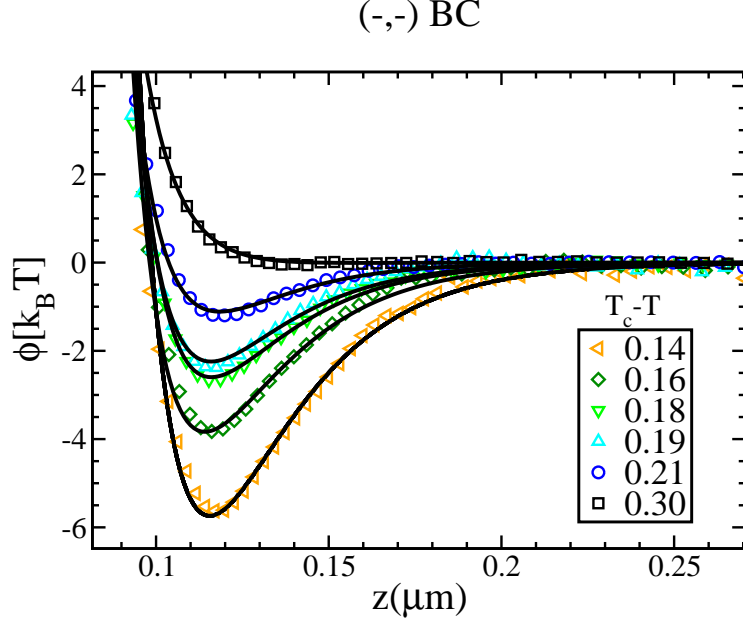


FIG. 4: (Color online) The effective potential between a wall and a colloidal particle of the radius  $R = 1200(nm)$  immersed in a water-lutidine mixture as a function of the distance  $z$  for various temperatures  $T$  [13]. The data refer to  $(-, -)$  BC corresponding to the case where both the colloidal particle and the substrate are hydrophilic. Here  $T_c$  is the critical temperature of the mixture. The solid lines are the theoretical predictions (Eqs. (70) and (62)) as explained in the main text. The parameters obtained from the fitting are shown in Table I.

We take into account that the wall-particle distance  $z$  was determined in experiments up to  $z_0 = \pm 30(nm)$ ; we assume that for the specific boundary condition (the same series of measurements) the shift between the actual and measured distance is fixed; the shift can differ from one series of measurements to another. In the fittings, we have tried to keep the same value for  $\xi_0$  for *all* sets of boundary conditions. The amplitudes  $\hat{A}_C = 2\pi A_{\pm}R$  have been taken from Ref. [13];  $A_+$  and  $A_-$  are the amplitudes governing the asymptotic decay ( $L/\xi \gg 1$ ,  $\tau > 0$ ) of the universal scaling functions of the critical Casimir force for symmetrical and antisymmetrical BC in a slit, respectively; for the Ising universality class in  $d = 3$ , the Casimir scaling functions in a slit geometry were obtained by MC simulation method in Ref. [21].

In Fig. 4, we show the comparison between our theoretical predictions, Eq. (70) with  $\Psi$  given by Eq. (62) (solid lines), and the experimental data of Ref. [13] for  $(-, -)$  BC. The obtained fit parameters are given in Table I. According to the table, the values of the

$T_c - T$	$\xi(nm)$	$\hat{A}_c(nm)$	$\sigma_0(nm)^{-2}$	$\sigma_L(nm)^{-2}$	$H_2(0)(nm)^{-3}$	$H_2(L)(nm)^{-3}$	$\kappa(nm)^{-1}$	$z_0(nm)$
0.14	25.9	-11379	1.28	0.064	-0.01	-0.0002	0.0872	-30
0.16	24.3	-11379	1.28	0.064	-0.01	-0.0002	0.09	-30
0.18	23.3	-11379	1.28	0.064	-0.01	-0.0002	0.091	-30
0.19	22.85	-11379	1.28	0.064	-0.01	-0.0002	0.0918	-30
0.21	21.24	-11379	1.28	0.064	-0.01	-0.0002	0.094	-30
0.30	16.3	-11379	1.28	0.064	-0.01	-0.0002	0.097	-30

TABLE I: Fit parameters for the effective potential given by Eqs. (70) and (62) for  $(-, -)$  BC where the colloidal particle with the radius  $R = 1200(nm)$  and the substrate are both hydrophilic. The amplitude  $\hat{A}_C$  for this system is taken from Ref.[13].  $\sigma_0$  and  $\sigma_L$  denote the surface charge at the particle and at the substrate respectively in units of elementary charge  $e$ .  $H_2(0)$  and  $H_2(L)$  denote respectively the dimensionless effective potential per unit volume between the particle and ions, and the flat substrate and ions (see Eqs.(37) and (44)).  $z_0$  is the experimental error in the measured distance between the substrate and the particle.  $\xi$  and  $\kappa$  are the correlation and the inverse Debye-length respectively. See the main text for more details.

correlation length

$$\xi = \xi_0^{fit} \left| \frac{T - T_c^{fit}}{T_c^{fit}} \right|^{-0.63} \quad (71)$$

with  $\xi_0^{fit} = 0.21 \pm 0.004(nm)$  and the Debye screening length  $\kappa^{-1} = 10.9 \pm 0.6(nm)$  are both in the range of the experimental results. The best fit is obtained for a zero shift in the critical temperature,  $T_c^{fit} = T_c$  but taking into account up to  $5mK$  inaccuracy in  $T$  itself. The charge density of the colloid (in units of the elementary charge  $e$ ) obtained from the fit is  $\sigma_0 = 1.28(nm)^{-2}$ , which agrees nicely with the value given in experiments of Refs. [29, 30], and is compatible with the observation that the highly charged colloids ( $\gtrsim 0.24(nm)^{-2}$ ) preferentially adsorb water while the colloids with a smaller amount of charge prefer lutidine.

Figure 5 shows the experimental data (symbols) and the theoretical curves (solid lines) for the case of  $(+, -)$  BC where the colloidal particle is hydrophobic whereas the wall is hydrophilic. The obtained fit parameters are given in Table II. According to the table, the amplitude of the correlation length and the Debye screening length are estimated as  $\xi_0^{fit} = 0.21 \pm 0.001(nm)$  and  $\kappa^{-1} = 10(nm)$ , respectively.  $H_2(L)$  and  $\sigma_L$  are the same as for

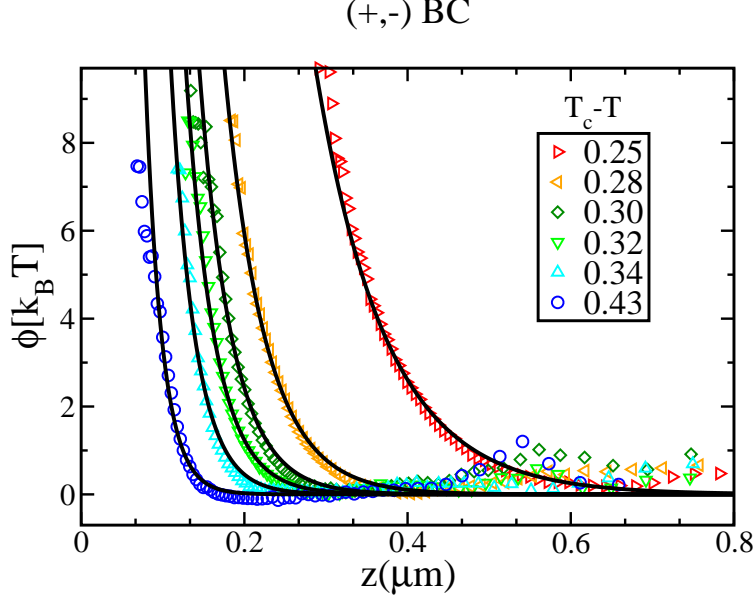


FIG. 5: (Color online) The same as in Fig. 4 but for  $(+, -)$  BC corresponding to the hydrophobic colloidal particle and the hydrophilic wall. The radius of the colloidal particle is  $R = 1850(nm)$ . The obtained parameters from the fitting are shown in Table II.

the  $(-, -)$  BC. In this case, the best fit is obtained with a shift in the critical temperature,  $\Delta T_c^{fit} \equiv |T_c - T_c^{fit}| = 223mK$  and allowing up to  $5mK$  inaccuracy in  $T$  itself. The charge density of the colloid (in units of  $e$ ) obtained from fitting is  $\sigma_0 = 0.7 \cdot 10^{-3}(nm)^{-2}$ , which is in agreement with Refs. [29] and [31] reporting the values for the surface charge densities of silica and polystyrene spheres in water.

Similarly, for  $(-, +)$  BC the comparison of the experimental data of [13] and our theoretical predictions for the effective potential are shown in Fig. 6. The obtained fit parameters are given in Table III. For this case, the estimates for the values of the amplitude of the correlation length and the Debye screening length are  $\xi_0^{fit} = 0.21 \pm 0.003(nm)$  and  $\kappa^{-1} = 10(nm)$ , respectively. As for the  $(-, -)$  BC, the best fit is obtained for considering no shift in the critical temperature,  $T_c^{fit} = T_c$ , and up to  $5mK$  inaccuracy in  $T$  itself. The charge densities and the surface fields of the colloidal particle and the substrate are consistent with the results of fitting for  $(-, -)$  BC.

For the experimental data corresponding to the  $(+, +)$  BC, i.e., where both the colloidal particle and the wall are hydrophobic, we find that  $1.1 \leq \kappa\xi \leq 2.1$  (see Table IV), which means that the approximation  $\kappa\xi \gg 1$  under which we have obtained Eq. (62) is not

$T_c - T$	$\xi(nm)$	$\hat{A}_c(nm)$	$\sigma_0(nm)^{-2}$	$\sigma_L(nm)^{-2}$	$H_2(0)(nm)^{-3}$	$H_2(L)(nm)^{-3}$	$\kappa(nm)^{-1}$	$z_0(nm)$
0.25	85.77	21144	0.0007	0.064	0.001	-0.0002	0.1	-18
0.28	49.5	21144	0.0007	0.064	0.001	-0.0002	0.1	-18
0.30	39.8	21144	0.0007	0.064	0.001	-0.0002	0.1	-18
0.32	34.8	21144	0.0007	0.064	0.001	-0.0002	0.1	-18
0.34	29.4	21144	0.0007	0.064	0.001	-0.0002	0.1	-18
0.43	20.5	21144	0.0007	0.064	0.001	-0.0002	0.1	-18

TABLE II: Fit parameters for the effective potential given in Eqs. (70) and (62) for  $(+, -)$  BC corresponding to the hydrophobic colloidal particle (with the radius  $R = 1850(nm)$ ) and the hydrophilic wall. The amplitude  $\hat{A}_C$  for this system is taken from Ref. [13]. For the remaining parameters see the caption of Table I.

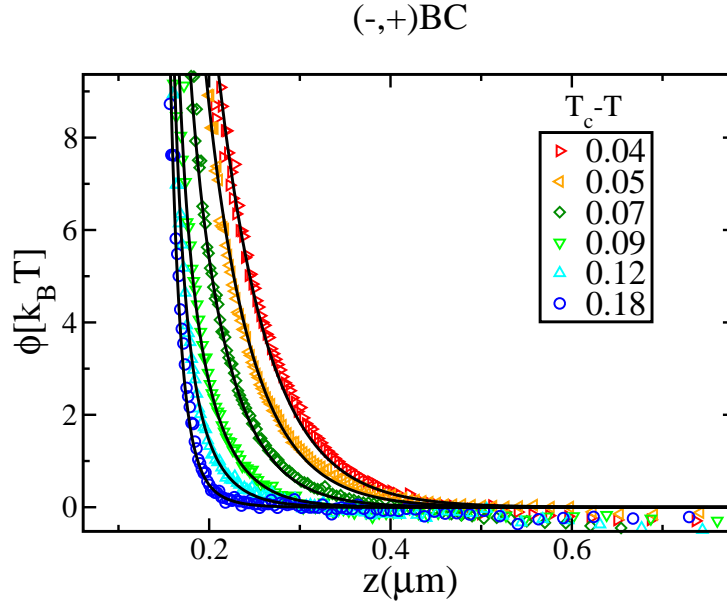


FIG. 6: (Color online) The same as in Fig. 4 but for  $(-, +)$  BC corresponding to the hydrophilic colloidal particle and the hydrophobic wall. The radius of the colloidal particle is  $R = 1200(nm)$ .

strictly valid. In this case, the terms which we have ignored in Eqs. (45) and (46) (the terms which decay as  $\exp(-2\kappa z)$ ) should be kept for a better comparison with the experiment. Nevertheless, we have performed fitting employing the relatively simple approximate form (62) of an effective potential. Because the neglected terms play a more significant role for small distances, in Fig. 7 we report the comparison with the experimental data only for

$T_c - T$	$\xi(nm)$	$\hat{A}_c(nm)$	$\sigma_0(nm)^{-2}$	$\sigma_L(nm)^{-2}$	$H_2(0)(nm)^{-3}$	$H_2(L)(nm)^{-3}$	$\kappa(nm)^{-1}$	$z_0(nm)$
0.04	55.07	13715	1.28	0.1344	-0.01	0.0001	0.1	30
0.05	50	13715	1.28	0.1344	-0.01	0.0001	0.1	30
0.07	42.5	13715	1.28	0.1344	-0.01	0.0001	0.1	30
0.09	34.64	13715	1.28	0.1344	-0.01	0.0001	0.1	30
0.12	29.64	13715	1.28	0.1344	-0.01	0.0001	0.1	30
0.18	23.50	13715	1.28	0.1344	-0.01	0.0001	0.1	30

TABLE III: Fit parameters for the effective potential given by Eqs. (70) and (62) for  $(-, +)$  BC, where the colloidal particle with radius  $R = 1200(nm)$  is hydrophilic while the substrate is hydrophobic. The amplitude  $\hat{A}_C$  for this system is taken from Ref. [13]. For more information see the caption of table I.

distances larger than  $z = 80(nm)$ . The obtained fit parameters are given in Table IV. According to the table our estimate for the amplitude of the correlation length is  $\xi_0^{fit} \simeq 0.21 \pm 0.018(nm)$  whereas for the Debye screening length we have  $\kappa^{-1} = 14.35 \pm 0.6(nm)$ . The smaller value obtained for  $\kappa$  for this BC indicates, according to Eq. (2), that the ion density  $\bar{\rho}_c$  is smaller compared to the other BC. Since the experiment was performed for  $\kappa\xi$  out of the range of validity of our approximate result, further studies for  $\kappa\xi \sim 1$  are required to verify whether the neglected terms in the potential would lead to the fit with  $\kappa^{-1} \sim 10nm$ . For the present case, the best fit is obtained with a shift in the critical temperature  $\Delta T_c^{fit} \equiv |T_c - T_c^{fit}| = 63mK$  and up to  $15mK$  inaccuracy in  $T$  itself. Again, the charge densities and surface fields of the colloidal particle and the substrate are consistent with the fitting parameters obtained for  $(-, +)$  and  $(+, -)$  boundary conditions respectively.

We find that the best fit for  $\xi_0$  for *all* BC is  $\xi_0 = 0.21(nm)$ . This value is in a very good agreement with several experimental results [32–36]. The correlation length  $\xi$  obtained from fits given in Tabs I-IV are compared with the expected behavior

$$\xi = \xi_0 \left| \frac{T - T_c}{T_c} \right|^{-0.63} \quad (72)$$

in Fig. 8.

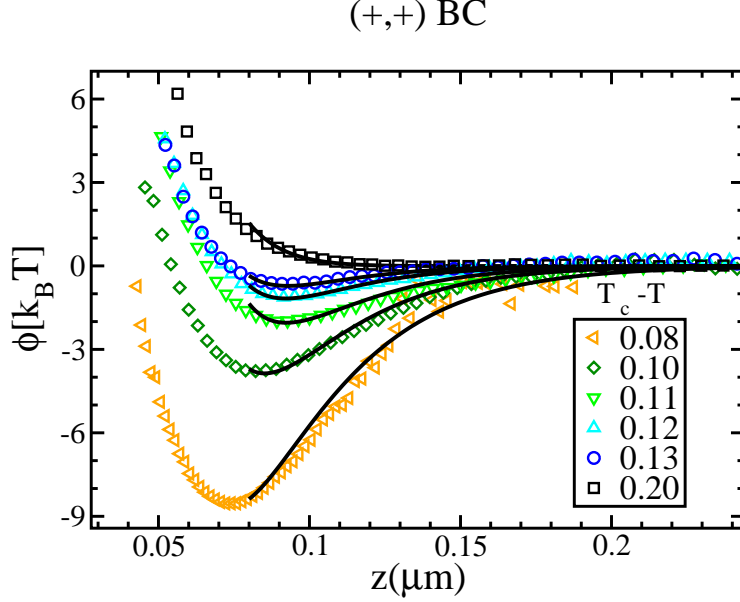


FIG. 7: (Color online) The same as in Fig. 4 but for (+,+) BC corresponding to hydrophobic both the colloidal particle and the wall. The radius of the colloidal particle is  $R = 1850(nm)$ . The obtained parameters from the fitting are shown in Table IV.

$T_c - T$	$\xi(nm)$	$\hat{A}_c(nm)$	$\sigma_0(nm)^{-2}$	$\sigma_L(nm)^{-2}$	$H_2(0)(nm)^{-3}$	$H_2(L)(nm)^{-3}$	$\kappa(nm)^{-1}$	$z_0(nm)$
0.08	30.1	-17543	0.0007	0.1344	0.001	0.0001	0.07	-15
0.1	25.93	-17543	0.0007	0.1344	0.001	0.0001	0.0675	-15
0.11	23.8	-17543	0.0007	0.1344	0.001	0.0001	0.0669	-15
0.12	21	-17543	0.0007	0.1344	0.001	0.0001	0.069	-15
0.13	19.3	-17543	0.0007	0.1344	0.001	0.0001	0.0708	-15
0.2	15.8	-17543	0.0007	0.1344	0.001	0.0001	0.0727	-15

TABLE IV: Fit parameters for the effective potential given by Eqs. (70) and (62) for (+,+) BC, where the colloidal particle with radius  $R = 1850(nm)$  and the substrate are both hydrophobic. Only the data larger than  $z = 80(nm)$  has been considered. The amplitude  $\hat{A}_C$  for this system is taken from Ref. [13]. For the remaining parameters see the caption of Table I.

## VII. SUMMARY AND DISCUSSION

In this paper we have studied a mutual effect of the critical adsorption and the distribution of ions on the effective potential between charged and selective surfaces confining a near-

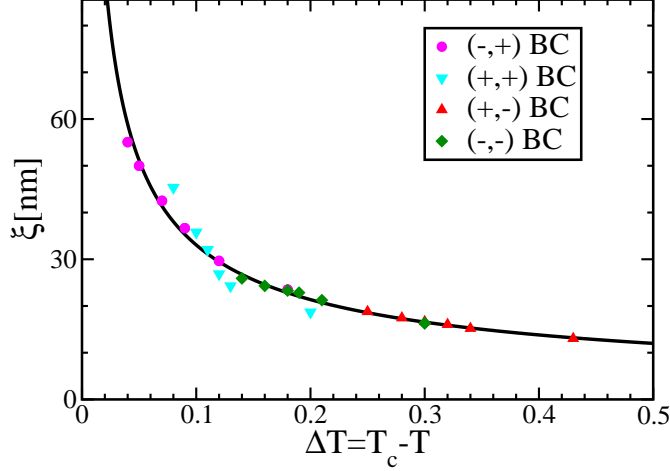


FIG. 8: The solid line shows the correlation length  $\xi$ , Eq. (72) with the amplitude  $\xi_0 = 0.21(nm)$  as a function of the deviation  $\Delta T = T_c - T$  from the critical temperature  $T_c$ . Symbols correspond to the best fits of the effective potential given by Eqs. (70) and (62) (Table I-IV). Recall that the case of  $(+,+)$  BC is out of range of validity of our approximation, and good agreement is not expected for this case.

critical binary mixture with ions. We have employed a Ginzburg-Landau-like theory which can be derived either from a lattice gas model [8] or from a simple density functional theory [9] for a four component mixture. We assumed the same chemical nature of the anion and the cation, and a much bigger solubility of the ions in a one component of a binary solvent than in the other. Such conditions are met, e.g., for aqueous solutions in which the ions come from a dissociation of a water. We have focused on the vicinity of the critical point of the solvent, where the correlation length for fluctuations of the solvent concentration,  $\xi$ , is much bigger than the screening length  $1/\kappa$ .

We have shown that when the chemical nature of the ions is the same, the excess grand potential of a system confined between two parallel walls can be split into two parts, a part which is independent of the charge distribution, and a part which is independent of the solvent concentration. The first contribution describes a near-critical binary solvent with a neutral solute (uncharged ions) comprised of single species with a preferential solubility in water. This part yields the critical Casimir potential. The second contribution to the excess grand potential is associated with the charge distribution, and has the form known from the DH theory. Both contributions, the critical Casimir and the DH, depend on the number density of ions. The equilibrium form of the number density of ions, corresponding

to the minimum of the grand potential, is different from that which arises from the critical Casimir part alone, and from the DH part alone. Thus, the effective potential between the confining walls differs from a sum of the Casimir potential in the uncharged system and the DH theory prediction for the electrostatic potential for ions in a homogeneous solvent.

We have shown that for  $\kappa\xi \gg 1$  the effect of the critical adsorption on the charge distribution dominates, and the effect of charges on the solvent concentration can be neglected [8]. This is because the screening length is much shorter than the correlation length, and the charges that are present at distances from the wall much smaller than  $\xi$  can be neglected, like the other molecular details. Because of the preferential solubility in water, the excess number density of ions decays in the same fashion as the excess solvent concentration, i.e.  $\sim \exp(-z/\xi)$ . The number density of ions determined by the critical adsorption is an input in calculations of the electrostatic contribution to the effective potential. It influences the charge distribution, and in addition changes the entropic contribution in the DH part of the grand potential. As a result we obtain terms which were absent in the standard DH potential in the case of the homogeneous solvent. The dominant additional terms are  $\sim \exp(-L/\xi)$  and  $\sim \exp(-\kappa L)$ .

Note that since the critical Casimir contribution to the excess grand potential has the same form as in the uncharged critical system and since for  $\kappa\xi \gg 1$  it can be considered independently of the remaining contribution to the excess grand potential, the RG theory can be applied to this part. Thanks to the above separation and thanks to the analytical solution, we have been able to incorporate in our theory the RG results for the critical Casimir part. The remaining electrostatic part was obtained on the MF level, with *correct* form of the number density of ions resulting from the critical adsorption. The key result of the RG theory is the universal form of the critical Casimir potential, depending only on the boundary conditions as discussed in the Introduction. The molecular details, described in this theory by the vdW interaction potentials, influence only the nonuniversal properties, in particular the amplitude  $\xi_0$  of the correlation function and the amplitude of the excess solvent concentration and the density of ions.

The dominant term in the electrostatic contribution to the excess grand potential decays in the same way as the critical Casimir potential. This electrostatic contribution is nonuniversal. Even though the critical Casimir part of the excess grand potential should exhibit the universal behavior, it can be obtained from experiments only when the electrostatic

contribution is subtracted.

In order to verify the theory, we have fitted our predictions to the experimental results [12, 13]. Two different substrates and two different particles were used in experiments to yield 4 combinations of the boundary conditions. We have kept the same values of parameters characterizing the same surface. This requirement has provided us a constraint on the fitting parameters for the surface charge and for the surface fields. We have used the Derjaguin approximation to take into account the curvature of the surface of the colloidal particle. We have obtained a good quantitative agreement for a large range of distances (Figs. 4-6) in three cases, and a less good agreement (Fig. 7) in the fourth case, which is at the limits of applicability of the approximations we have made. In our fitting, the amplitude  $\xi_0 = 0.21nm$  has the same value for all the considered cases, and this value is in a very good agreement with various experimental estimates [32–36]. The best fit is obtained for the correlation length that agrees very well with the expected behavior (see Fig. 8) (except from the boundary conditions  $(+, +)$ , where the agreement is less good). Also the fitted value of the critical temperature was precisely equal to the experimental value for  $(-, -)$  and  $(-, +)$  BC, with small shifts,  $\Delta T_c = 63mK$  and  $\Delta T_c = 223mK$ , for the  $(+, +)$  and  $(+, -)$  BC, respectively.

As already mentioned in the Introduction, the attempt to fit experimental results reported in Ref. [12, 13] to the sum of the critical Casimir and the electrostatic potentials failed. Moreover, in order to fit the experimental results to the universal Casimir potential for large separations, a different value of  $\xi_0$  had to be chosen for each BC, from  $0.17nm$  to  $0.26nm$  for  $(-, -)$  and  $(-, +)$  BC respectively, and the  $(+, +)$  BC could not be fitted to the Casimir potential alone. A smaller value of  $\xi_0$  leads to a larger prefactor  $\hat{A}_C/\xi$  multiplying the exponential decay  $\exp(-L/\xi)$  of the potential. In the present theory the prefactor of the decay  $\exp(-L/\xi)$  contains the electrostatic contribution in addition to the universal Casimir amplitude. Therefore both, the present theory with  $\xi_0 = 0.21nm$  and the pure critical Casimir potential with  $\xi_0 = 0.17nm$  can yield a good fit at large distances for  $(-, -)$  BC. However, unlike in the present approach, the other BC could not be fitted by the critical Casimir potential alone with the same value of  $\xi_0$ , and the relative difference between the fitted amplitudes was as large as  $(0.26 - 0.17)/0.17 > 50\%$ . We cannot find explanation for such large differences in the amplitudes for essentially the same mixtures. Boundary conditions should not have any effect on the bulk properties. Moreover, in Ref. [12, 13] only

distances much larger from the position of the potential minimum could be fitted, whereas the present theory yields a good quantitative agreement for a wide range of distances. The agreement is obtained for all the measured systems for the parameters that agree very well with the experimental data, and if precise experimental data are absent, are of a correct order of magnitude. There are no data for the surface fields of the four surfaces. The four free parameters, however, satisfy all the constraints of consistency for the four pairs of surfaces (24 curves in 4 series of measurements).

We conclude by stressing that a very important advantage of the analytical expression (Eqs.(62)-(65)) is the possibility of designing the effective potential of a desired form by adjusting the surface charges and/or hydrophilicity (or hydrophobicity) of the surfaces, or the amount of ions in the solution. Eq.(62) may be a very useful tool in guiding future experimental studies.

### Acknowledgments

We have greatly benefited from discussions with Siegfried Dietrich, Ursula Nellen, Marcus Bier and especially Laurent Helden, who explained us the details of experiments and commented on the results of fitting. Faezeh Pousaneh would like to thank Prof. Dietrich and his group for hospitality during her stay in Stuttgart, where a part of this work was done. The work of Faezeh Pousaneh was realized within the International PhD Projects Programme of the Foundation for Polish Science, cofinanced from European Regional Development Fund within Innovative Economy Operational Programme "Grants for innovation".

### VIII. APPENDIX A. EXPLICIT EXPRESSIONS FOR $C_{ij}^0$

The coefficients in Eq. (29) take the explicit forms

$$C_{ss}^0 = k_B T \frac{1 - \bar{\rho}_c}{(1 - \bar{\rho}_c)^2 - \bar{s}^2} - 6J_{ss} \quad (73)$$

$$C_{\rho\rho}^0 = k_B T \left( \frac{1 - \bar{\rho}_c}{(1 - \bar{\rho}_c)^2 - \bar{s}^2} + \frac{1}{\bar{\rho}_c} \right) - 6J_{\rho\rho} \quad (74)$$

$$C_{s\rho}^0 = C_{\rho s}^0 = k_B T \frac{\bar{s}}{(1 - \bar{\rho}_c)^2 - \bar{s}^2} - 6J_{\rho s}. \quad (75)$$

## IX. APPENDIX B. EXPLICIT EXPRESSIONS FOR THE COEFFICIENTS IN EQ. (49)

The coefficients in Eq. (49) take the explicit forms

$$\mathcal{A}_0 = \left( \frac{\mathcal{A}_{00}}{y+1} \right) \left[ 1 - y \frac{(1 - e^{-L/\xi})}{1 - e^{-\kappa L}} e^{-\kappa L} \right] - \left( \frac{\mathcal{A}_{0L}}{y-1} \right) \left[ 1 - y \frac{1 - e^{-L/\xi}}{1 - e^{-\kappa L}} \right] \quad (76)$$

and

$$\mathcal{A}_L = \left( \frac{\mathcal{A}_{LL}}{y+1} \right) \left[ 1 - y \frac{(1 - e^{-L/\xi})}{1 - e^{-\kappa L}} e^{-\kappa L} \right] - \left( \frac{\mathcal{A}_{L0}}{y-1} \right) \left[ 1 - y \frac{1 - e^{-L/\xi}}{1 - e^{-\kappa L}} \right] \quad (77)$$

where

$$\mathcal{A}_{00} = n_0 \frac{(y+1)^2}{(2y+1)}, \quad (78)$$

$$\mathcal{A}_{0L} = -n_L \frac{(y-1)^2}{(2y-1)} \quad (79)$$

$$\mathcal{A}_{L0} = -n_0 \frac{R_\sigma (y-1)^2}{(2y-1)} \quad (80)$$

$$\mathcal{A}_{LL} = n_L \frac{R_\sigma (y+1)^2}{(2y+1)} \quad (81)$$

Note that each coefficient (78)-(81) diverges for  $y = \kappa\xi \rightarrow \infty$ . However, the term  $\mathcal{A}_{00}e^{-\kappa z}(1 - e^{-z/\xi})$  in (49) remains finite, because when  $\kappa \rightarrow \infty$  then  $ye^{-\kappa z} \rightarrow 0$ , and when  $\xi \rightarrow \infty$  then  $y(1 - e^{-z/\xi}) \simeq yz/\xi = \kappa z$ . Likewise, the whole correction to the charge profile, Eq. (49), is finite.

## X. APPENDIX C. EXPLICIT FORM OF THE LEADING-ORDER CORRECTION TERM EQ. (57)

Full expression for the  $\mathcal{L}_{el}^{(2)}$  in Eq. (57) has following form

$$\mathcal{L}_{el}^{(2)} = \frac{k_B T \kappa \sigma_0^2}{2\bar{\rho}_c^2} \hat{\mathcal{L}}_{el}^{(2)} \quad (82)$$

where

$$\hat{\mathcal{L}}_{el}^{(2)} = \left\{ \frac{2y(1 - R_\sigma)e^{-\kappa L}}{(1 - e^{-\kappa L})^2} \left( \frac{(n_0 - R_\sigma n_L)(1 - e^{-\kappa L}e^{-L/\xi})}{2y + 1} - \frac{(n_L - n_0 R_\sigma)(e^{-\kappa L} - e^{-L/\xi})}{2y - 1} \right) \right. \\ \left. - \frac{y(1 - e^{-L/\xi})}{(1 - e^{-\kappa L})^2} \left( 2R_\sigma(n_0 + n_L)e^{-\kappa L} + \frac{(n_0 + n_L R_\sigma^2)}{2y + 1}e^{-2\kappa L} - \frac{(n_L + n_0 R_\sigma^2)}{2y - 1} \right) \right. \\ \left. + \left( \frac{-2(n_0 + n_L)(1 + R_\sigma^2)y^2 + (n_0 - n_L)(1 - R_\sigma^2)y}{4y^2 - 1} \coth\left(\frac{\kappa L}{2}\right) + \frac{y(n_0 + n_L R_\sigma^2)}{2y + 1} \right) \right\} \quad (83)$$

and the expressions for  $n_0$  and  $n_L$  are given in Eq. (42).

- 
- [1] E. L. Eckfeldt and W. W. Lucasse, J. Phys. Chem. **47**, 164 (1943).
  - [2] B. J. Hales, G. L. Bertrand and L. G. Hepler, J. Phys. Chem. **70**, 3970 (1966).
  - [3] A. Onuki and H. Kitamura, J. Chem. Phys. **121**, 3143 (2004).
  - [4] A. Onuki and R. Okamoto, Curr. Opin. Colloid In. **16**, 525 (2011).
  - [5] Y. Tsori and L. Leibler, Proc. Nat. Acad. Sci. USA **104**, 7348 (2007).
  - [6] D. Ben-Yaakov, D. Andelman, D. Harries and R. Podgornik, J. Phys. Chem. B **113**, 6001 (2009).
  - [7] for recent reviews on ion-specific effects in aqueous solutions see: D. Ben-Yaakov, D. Andelman, D. Harries and R. Podgornik, J. Phys.: Condens. Matter **21**, 424106 (2009); D. Ben-Yaakov, D. Andelman, R. Podgornik and D. Harries, Curr. Opin. Colloid In. **16**, 542 (2011).
  - [8] A. Ciach and A. Maciolek, Phys. Rev. E **81**, 041127 (2010).
  - [9] F. Pousaneh and A. Ciach, J. Phys.: Condens. Matter **23**, 412001 (2011).
  - [10] M. Bier, A. Gambassi, M. Oettel and S. Dietrich, EPL **95**, 60001 (2011).
  - [11] S. Samin and Y. Tsori, EPL **95**, 36002 (2011).
  - [12] C. Hertlein, L. Helden, A. Gambassi, S. Dietrich, and C. Bechinger, Nature **451**, 172 (2008).
  - [13] A. Gambassi, A. Maciolek, C. Hertlein, U. Nellen, L. Helden, C. Bechinger and S. Dietrich, Phys. Rev. E. **80**, 061143 (2009).
  - [14] U. Nellen, J. Dietrich, L. Helden, S. Chodankar, K. Nygard, J. F. van der Veen, and C. Bechinger Soft Matter **7**, 5360 (2011).

- [15] M. E. Fisher and P. G. de Gennes, C. R. Acad. Sci. Ser. B **287**, 207 (1978).
- [16] M. Krech, *Casimir Effect in Critical Systems* (World Scientific, Singapore, 1994); J. Phys.: Condens. Matter **11**, R391 (1999).
- [17] G. Brankov, N. S. Tonchev, and D. M. Danchev, *Theory of Critical Phenomena in Finite-Size Systems* (World Scientific, Singapore, 2000).
- [18] More recent results for critical Casimir forces are summarized in A. Gambassi, J. Phys.: Conf. Ser. **161**, 012037 (2009).
- [19] S. Samin and Y. Tsori, arXiv:1201.3535v1
- [20] B. Derjaguin, Kolloid Zeitschrift **69**, 155 (1934).
- [21] O. Vasilyev, A. Gambassi, A. Maciołek, and S. Dietrich, Europhys. Lett. **80**, 60009 (2007)
- [22] K. Sadakane, A. Onuki, K. Nishida, S. Koizumi, and H. Seto, Phys. Rev. Lett. **103**, 167803 (2009).
- [23] H. W. Diehl, in *Phase Transitions and Critical Phenomena*, edited by C. Domb and J. L. Lebowitz (Academic, London, 1986), Vol. 10, p. 76.
- [24] R. Evans, J. Phys.: Condens. Matter **2**, 8989 (1990); and references therein.
- [25] (a) M. N. Barber in *Phase Transitions and Critical Phenomena*, edited by C. Domb and J. L. Lebowitz (Academic, New York, 1983), Vol. 8, p. 149; (b) V. Privman, in *Finite Size Scaling and Numerical Simulation of Statistical Systems*, edited by V. Privman (World Scientific, Singapore, 1990), p. 1.
- [26] D. Ben-Yaakov, D. Andelman, and R. Podgornik, J. Chem. Phys **134**, 074705 (2011).
- [27] J. N. Israelachvili, *Intermolecular and Surface Forces*, (Academic, London, 1992).
- [28] J.-L. Barrat and J.-P. Hansen, *Basic concepts for simple and complex liquids* (Cambridge University Press, Cambridge, 2003).
- [29] P. D. Gallagher and J. M. Maher, Phys. Rev. A **46**, 2012 (1992).
- [30] P. D. Gallagher, M. L. Kurnaz, and J. V. Maher, Phys. Rev. A **46**, 7750 (1992).
- [31] H. H. von Grunberg, L. Helden, P. Leiderer, and C. Bechinger, J. Chem. Phys. **114**, 10094 (2001).
- [32] S. Z. Mirzaev, R. Behrends, T. Heimbürg, J. Haller, and U. Kaatz, J. Chem. Phys. **124**, 144517 (2006).
- [33] E. Güleri, A. F. Collings, R. L. Schmidt, and C. J. Pings, J. Chem. Phys. **56**, 6169 (1972).
- [34] M. Jungk, L. Belkoura, D. Woermann, and U. Würz, Ber. Bunsenges. Phys. Chem. **91**, 507

(1987).

[35] L. V. Entov, V. A. Levchenko, and V. P. Voronov, *Int. J. Thermophys.* **14**, 221 (1993).

[36] D. S. P. Smith, B. M. Law, M. Smock, and D. P. Landau, *Phys. Rev. E* **55**, 620 (1997).